LIF Spectra of Cyclohexoxy Radical and Direct Kinetic Studies of Its Reaction with O_2

Lei Zhang, Katherine A. Kitney, Melissa A. Ferenac, Wei Deng, and Theodore S. Dibble*

Department of Chemistry, SUNY—Environmental Science and Forestry, 1 Forestry Drive, Syracuse, New York 13210

Received: September 28, 2003; In Final Form: November 12, 2003

The laser-induced fluorescence (LIF) excitation spectrum of cyclohexoxy radical has been measured for the first time. The dominant vibrational progression is consistent with computations, at CIS/6-31+G(d), of the C−O stretch frequency of the axial conformer of cyclohexoxy radical. LIF intensity was used as a probe in direct kinetic studies of the reaction of cyclohexoxy radicals with O_2. The Arrhenius expression obtained was $k_{O2} = (5.8 \pm 2.3) \times 10^{-12}$ exp[(−14.3 ± 0.8) kJ/mol/*RT*] cm^3 molecule^{-1} s^{-1} (225−302 K), independent of pressure in the range 50−125 Torr. The room temperature rate constant for this reaction is a factor of 2 higher than the commonly recommended value, but the observed activation energy is 9 times larger than the recommended value of 1.6 kJ/mol. Combining our results with the ratio of rate constants, $k_{O2}/k_{scission}$, measured in chamber experiments, we obtained an Arrhenius expression for $k_{scission}$, the rate constant for β C−C scission of cyclohexoxy radical. However, the resulting Arrhenius preexponential factor of 4.5×10^{15} s^{-1} is unreasonably high compared with the value of $\sim 2 \times 10^{13}$ s^{-1} obtained in our RRKM/Master Equation calculations as well as in calculations and experiments reported for other alkoxy radicals. The apparent discrepancy is resolved by examining the uncertainties in the values of $k_{scission}$ and the limited temperature range spanned by the relative rate experiments. A part of the discrepancy might also be explained by the observation that the O_2 rate constant measured here is only for a single conformer of cyclohexoxy radical, whereas the relative rate experiments represent some averaging over both conformers.

I. Introduction

The formation of ozone and organic aerosols in polluted air is controlled by the degradation of volatile organic compounds (VOCs). Alkoxy radicals are important intermediates in the degradation of most VOCs.[1] The atmospheric fate of large alkoxy radicals ($\geq C_4$) is usually determined by competition among β C−C scission, reaction with O_2, and isomerization,[2] as shown in Scheme 1. Each reaction pathway contributes differently to the formation of ozone and secondary organic aerosols.[3] Therefore, understanding alkoxy radical chemistry in the atmosphere is of crucial importance for understanding and modeling smog chemistry.

Vehicle exhaust and evaporation of gasoline are important sources for the emission of alkanes and cycloalkanes in urban areas. Cyclohexane constitutes 0.1−1.0 wt % of the gasoline sold in the U.S., Germany, and the U.K.[4] In the polluted troposphere, alkanes and cycloalkanes react with OH• in the presence of O_2 and NO to form alkoxy radicals. The kinetics of small, acyclic alkoxy radicals have received much attention, but, although there are several smog chamber studies inferring information about cyclohexoxy radicals,[5−8] there have been no direct studies of any gas-phase alkoxy radicals containing a six-membered ring. This is a significant gap because the most abundantly emitted terpenes (alkenes with molecular formula $C_{10}H_{16}$) possess six-membered rings; terpenes are very important in atmospheric chemistry due to their large emissions and their role in aerosol formation. Kinetic studies of cyclohexoxy radicals may provide insight into the chemistry of alkoxy radicals from terpenes.

SCHEME 1

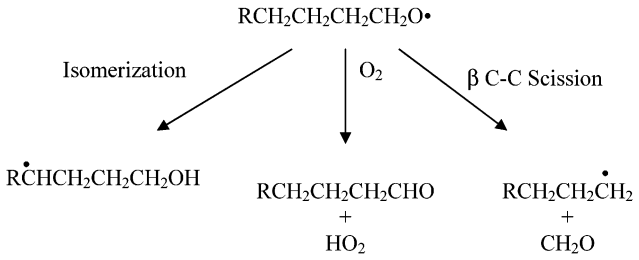

Although alkoxy radicals in general can react via three channels in the atmosphere, isomerization of the cyclohexoxy radical is slow in comparison to β C−C scission and reaction with O_2. This is attributed to the high energy of the boat-twist conformation required for the transition state for isomerization.[7] Reaction of cyclohexoxy radical with O_2 to produce cyclohexanone competes with the β C−C scission reaction under atmospheric conditions (cyclohexanone yield 25−35%).[5−8]

The technique of laser-induced fluorescence (LIF) has long been used to monitor small alkoxy radicals (C_1–C_3) in direct kinetic studies due to its excellent sensitivity, selectivity, and time resolution.[9−18] More recently, spectroscopic and kinetic investigations have been extended to larger alkoxy radicals,[19−25] and spectroscopic experiments of many of these larger alkoxy radicals have been carried out under jet-cooled conditions.[26−28] Due to the lack of any LIF (or other) spectra for cyclohexoxy radical, there have been no direct studies of its reaction kinetics.

This paper first discusses the experimental and computational methods employed. Next the LIF excitation spectrum of cyclohexoxy radical is presented, followed by computational results on the relative energies of the conformers of cyclohexoxy

* To whom correspondence should be addressed. FAX: (315) 470-6856. E-mail: tsdibble@syr.edu.

10.1021/jp036891p CCC: $27.50
Published on Web 12/23/2003

and the vibrational spectra of their second excited ($\tilde{B}$) states. The discussion then turns to the absolute rate constant, k_{O2}, for the reaction of cyclohexoxy radical with O_2 versus temperature (and pressure). The calculated rate constant for β C−C scission is presented and compared to that inferred from relative rate experiments using both the previously recommended and the present results for k_{O2}. Finally, discrepancies arising from these comparisons are discussed.

II. Experimental and Theoretical Methods

An excimer (GAM Laser, Inc., EX100H) laser operating at 351 nm was used to photolyze cyclohexyl nitrite and generate the cyclohexoxy radical. A dye laser (Lambda Physik, FL3002) pumped by another excimer laser (Lambda Physik, Lextra 100, 308 nm) was used to excite the radicals. The beams of the two lasers counter-propagated through the cell in most experiments, but a few experiments were carried out with the two lasers perpendicular to each other. The delay time between the dye laser and the photolysis laser is adjusted by a digital delay generator. The lasers were operated at 2 Hz. The fluorescence signal is converted into electric signal by a PMT perpendicular to both lasers. The electric signal is monitored by a boxcar that transfers a digital signal to a computer for data acquisition. The gate width on the boxcar used to record the signal intensities is 20 ns, and the gate is delayed by 70 ns with respect to the scattered light.

LIF spectra of cyclohexoxy were obtained at 226 K in N_2 buffer gas by measuring the integrated fluorescence signal intensity while continuously scanning the excitation laser wavelength at 0.03 nm/s. The spectral ranges were 345−370 and 363−403 nm covered by the laser dyes DMQ and PPI, respectively. We verified that the spectrum only appeared in the presence of the photolysis laser and that the signal strength decreased significantly when the delay time between the photolysis and excitation lasers were extended from 5 to 300 μs; both observations suggest the reported spectra are due to radicals produced by cyclohexyl nitrite photolysis rather than wall reactions or secondary chemistry. All the spectral intensities were corrected by subtracting the background obtained with the photolysis laser blocked and normalized by dividing by the laser power. Flow rates and pumping rates were fixed in all spectroscopic experiments to maintain 13 mTorr partial pressure of cyclohexyl nitrite and 50 Torr total pressure (at 226 K).

In the kinetic experiments, the dye laser was fixed at one of four different excitation wavelengths: 349.749, 356.161, 373.586, and 374.460 nm. These wavelengths are marked by a star in Figure 1. The pseudo-first-order rate constants for radical loss were determined from the rate of change of the signal intensity with delay time. We recorded signal intensities at 16 different delay times ranging from 5 μs to 10 ms. At each delay time 100 measurements were made and averaged. The partial pressure of cyclohexyl nitrite was maintained at 13 mTorr in most experiments. Recently, we have improved the signal-to-noise ratio sufficiently that we can carry out experiments with about one-third the concentration of cyclohexyl nitrite (and cyclohexoxy radical), and rate constants were remeasured at three temperatures using this lower cyclohexyl nitrite concentration.

Cyclohexyl nitrite was synthesized by the dropwise addition of a mixture of sulfuric acid and cyclohexanol to an aqueous sodium nitrite solution[29] and purified by trap-to-trap distillation. FTIR[30] and NMR[30] spectra were obtained to verify the structure and purity of the product. Based on the NMR experiment, the major impurity (~13%) in the nitrite sample was found to be cyclohexanol, which does not produce any fluorescence at the wavelengths used in our experiment. The liquid nitrite sample was kept at −20 °C when not in use. In the experiment, the gas mixture was prepared by diluting the vapor of nitrite precursor to a mole fraction of 1% (or 0.3%) in N_2 (Haun Welding Supplies, 99.999%) in a 10-L darkened glass bulb at room temperature.

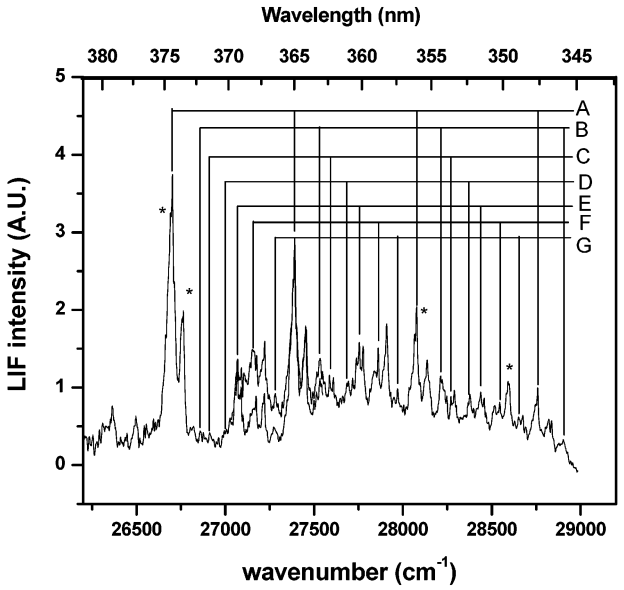

Figure 1. Laser-induced fluorescence (LIF) spectrum of cyclohexoxy radical at 226 K and 50 Torr N_2. Peaks used in the kinetics experiments are marked with an asterisk.

To estimate the concentration of cyclohexyl nitrite photolyzed, we carried out a single measurement of the UV spectrum of cyclohexyl nitrite in a 10-cm Pyrex cell with quartz windows. The resultant (approximate) absorption cross section at 351 nm was 1.8×10^{-19} cm^2. Using this value and the photolysis laser fluence of 20 mJ/cm^2, we estimate the initial alkoxy radical concentration to be 5.2×10^{12} molecules/cm^3 (or 1.7×10^{12} molecules/cm^3 at the lower cyclohexyl nitrite concentration). The temperature of the gases inside the cell was varied between 225 and 302 K. The partial pressure of O_2 (Messer, 99.999%) varied from 0.7 Torr (2.3×10^{16} molecules/cm^3 at 298 K) to 4.0 Torr. The high partial pressure of O_2 ensures that the kinetic experiments are carried out under pseudo-first-order conditions. N_2 was added to set the total pressure at 50 Torr (or 125 Torr in a few experiments).

Temperatures of gases in the cell were measured by a Type T thermocouple located 1−2 cm below the height of the laser beams at the point where the fluorescence is monitored. At 50 Torr and 225 K, the displacement of the thermocouple from the center of the flow results in reported temperatures that understate the gas temperature in the relevant volume by 2 deg. The error is less than 2 deg at all other temperatures used in these experiments.

Quantum calculations employed the Gaussian98 series of programs[31] and examined both conformers of cyclohexoxy radical. All radicals were treated with the spin-unrestricted formalism. Different computational methods were used for different purposes. The relative energy of the axial and equatorial conformers was studied by second-order Møller−Plesset perturbation theory (MP2) with all orbitals correlated. MP2 theory, unlike most density functional approaches, includes a good representation of dispersion forces, which are critical to determining the energy difference between the conformers. Harmonic vibrational frequencies were computed with the geometry optimized using the 6-31G(d,p) basis set, and elec-

TABLE 1: Absolute Energies (Hartrees), Zero Point Energies (in parentheses, kJ/mol), and Relative Energies (kJ/mol) of Axial and Equatorial Conformers of the Cyclohexoxy Radical

	equatorial		axial	
level of theory	absolute energy	relative energy	absolute energy	relative energy
B3LYP/6-31G(d,p)	−310.441 30 (421.5)	0	−310.440 68 (421.5)	1.7
B3LYP/6-311G(2df,2p)	−310.527 19	0	−310.526 76	1.2
MP2/6-31G(d,p)	−309.482 46 (436.1)	0	−309.482 48 (436.3)	0.1
MP2/6-311++G(2d,2p)	−308.536 05	0	−308.534 94	3.1

tronic energy differences were refined by reoptimizing the geometry using the 6-311++G(2d,p) basis set.

We carried out computations on the β C−C scission reaction of cyclohexoxy radical because of its importance to the atmospheric fate of cyclohexoxy and to help determine the Arrhenius preexponential factor independently of experiment. To characterize the C−C scission reaction we used density functional theory, specifically, the correlation functional of Lee, Yang, and Parr combined with the three-parameter HF exchange functional of Becke (B3LYP).[32,33] The basis sets used were 6-31G(d,p) and 6-311G(2df,2p). B3LYP, unlike MP2, has been fairly successful in computing activation barriers to β C−C scission reactions of alkoxy radicals, especially with the 6-31G(d,p) basis set.[34−37] We carried out RRKM/Master Equation calculations using the UNIMOL program[38] and the B3LYP/6-31G(d,p) relative energies to compute the rate constants for β C−C scission at a range of temperatures and pressures. These computations enable us to calculate the corresponding activation energies and Arrhenius preexponential factors.

The reaction of alkoxy radicals with O_2 presents some difficulties which preclude a calculation as part of this paper. It has been shown that the O_2 reaction of alkoxy radicals involves a highly spin-contaminated transition state, for which CASSCF calculations may be necessary.[39] Moreover, the reaction rate is highly sensitive to tunneling and the detailed dynamics.[39,40]

To characterize the vibrational structure of the excited state of cyclohexoxy radical we employed the method of configuration interaction with single excitations (CIS) with the 6-31+G(d) basis set. This method has been fairly successful in previous analyses of alkoxy radical vibrational spectra.[26] The adiabatic excitation energies from CIS are not reported because they are expected to be less accurate than empirical estimates based on experimental results for other secondary alkoxy radicals.[20,26]

III. Results and Discussion

1. LIF Detection of Cyclohexoxy Radical. Figure 1 shows the fluorescence excitation spectrum of cyclohexoxy radicals from 345 to 403 nm at 226 K and 50 Torr total pressure. Note that Figure 1 shows two overlapping spectra using different dyes; large intensity differences in the region of overlap are due to errors in normalizing the spectra in the wings of the tuning curves of the two laser dyes. Four pairs of peaks, split by ∼60 cm^{-1}, are found in the dominant progression (marked as A in Figure 1) starting at 26 702 cm^{-1}. Note that the apparent origin bands of secondary alkoxy radicals fall at about 26500 ± 250 cm^{-1},[20,26] so the strong peak at 26 702 cm^{-1} or the two weaker peaks to the red are consistent with the expected location of the origin band. In progression A, the intervals are 689, 686, and 682 cm^{-1}. The intensity of peaks decreases with the increasing wavenumber. No obvious progression was found involving peaks at lower energy than 26 702 cm^{-1}. In addition to progression A, there are six reproducible progressions which also possess ∼685-cm^{-1} intervals. The apparent origins of these transitions are displaced to higher frequency with respect to each peak in progression A: progression B with four (triplet) peaks, ∼135 cm^{-1} higher; progression C with three (doublet) peaks, ∼193 cm^{-1} higher; progression D with three (doublet) peaks, ∼290 cm^{-1} higher; progression E with three (triplet) peaks, ∼361 cm^{-1} higher; progression F with three strong (triplet) peaks, ∼458 cm^{-1} higher; and progression G with three (triplet) peaks, ∼575 cm^{-1} higher. It is reasonable to identify these progressions as possessing between zero and three quanta in the mode with frequency ∼685 cm^{-1} and one quantum of excitation in one of several different modes (with frequencies of ∼135, ∼193, ∼290, ∼361, ∼458, and ∼575 cm^{-1}. However, this assignment cannot be confirmed without better-resolved (i.e., jet-cooled) spectra as well as an understanding of possible confounding factors (e.g., excitation out of the vibrationally excited ground state, axial vs equatorial conformers).

Cyclohexoxy radical possesses two dominant conformers, axial and equatorial,[41] as shown below.

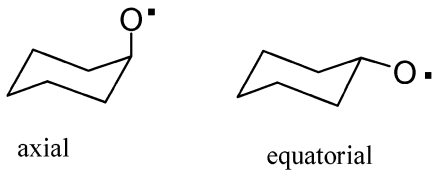

axial equatorial

The MP2/6-311++(2d,2p) calculations indicate that the equatorial conformer is more stable than the axial conformer by 3.1 kJ/mol (see Table 1). The other calculations also favor the equatorial conformer, albeit to lesser extents. The structure obtained for the equatorial conformer possesses C_s symmetry and an A′ ground state.

The C−O stretch mode typically dominates the near-ultraviolet ($\tilde{B}$ state) spectra of alkoxy radicals because the C−O bond distance in the excited state is extended by 0.1−0.25 Å over the ground-state value.[42,43] Most alkoxy radical spectra show strong progressions from C−O stretch modes with vibrational frequencies in the range 520−600 cm^{-1}.[26,44−49] However, recent analyses suggest that conformers of linear alkoxy radicals may possess C−O stretch frequencies as high as 671−676 cm^{-1}.[27,28] Therefore, our analysis of the computations on the excited-state focuses on the modes with C−O stretch character and modes in the region 520−700 cm^{-1}. Our CIS/6-31+G(d) calculations on the A′$\tilde{B}$ state of the equatorial conformer indicated that the C−O stretch mode was at 817 cm^{-1}, which is very different from that found for other alkoxy radicals or in our experiments. A vibrational mode of A′ symmetry with significant C−O stretch component was also found at 574 cm^{-1} (similar to the C−O stretch mode frequency in other alkoxy radicals) but this mode was dominated by a CCC bending motion. The calculated vibrational frequencies suggest that the equatorial conformer of cyclohexoxy radical do not include any modes between 574 and 817 cm^{-1}. Therefore, the calculations appear inconsistent with the observed ∼685-cm^{-1} interval which dominates the observed LIF spectrum.

We optimized a $\tilde{B}$ state of A′ symmetry for the axial conformer of cyclohexoxy at CIS/6-31G(d,p), but it had one

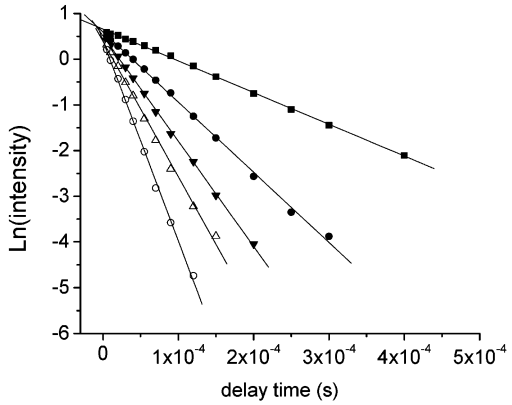

Figure 2. Typical linear decay of ln(LIF intensity) as a function of the delay time for cyclohexoxy reacting with O_2 at total pressure 50 Torr and 268 K. O_2 concentrations in molecules/cm^3 are, ■ 1.6×10^{14}, ● 3.1×10^{14}, ▲ 4.7×10^{14}, △ 6.3×10^{14}, and ○ 8.5×10^{14}.

imaginary frequency. When symmetry was relaxed, we optimized a structure with near-C_s symmetry. Unfortunately, the frequency calculations did not converge in several attempts. We present here the results of J. Liu, who graciously allowed us to report his results prior to his submitting them for publication.[50] His results show modes with C−O stretch character at 812 cm^{-1} (A″) and 694 cm^{-1} (A′). The presence of a mode near 690 cm^{-1} in the computed spectrum of the axial conformer and its absence in the calculated spectrum of the equatorial conformer suggest that the dominant features in the experimental spectrum should be assigned to the axial conformer. Further investigation is needed before one can be confident in this assignment.

2. The Reaction of Cyclohexoxy Radical with O_2. The reaction with O_2 is considered to be a major pathway for the degradation of cyclohexoxy radical in the atmosphere.[2]

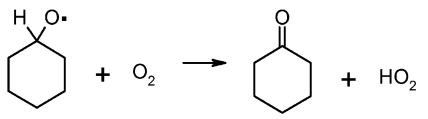

(1)

Figure 2 shows a typical plot of the natural logarithm of LIF intensity versus delay time for cyclohexoxy reacting with various concentrations of O_2. The slopes of each of the lines in Figure 2 represents a pseudo-first-order rate constant for loss of cyclohexoxy radical. We note here that vibrational structure of the spectrum does not change with delay time, so that there is no significant fluorescence from the products of reaction 1 or other reactions. Bimolecular reaction rate constants were obtained from the slopes of the linear correlation between the pseudo-first-order rate constant and different concentrations of O_2 in the experiments, as shown in Figure 3. The high linearity of the data shown in Figures 2 and 3 confirms that the pseudo-first-order approximation is valid here. The rate constant at 301 K (averaged over two determinations) is $(2.1 \pm 0.5) \times 10^{-14}$ cm^3 molecule^{-1} s^{-1}, which is 2.6 times greater than the suggested 298 K value for all secondary alkoxy radicals:[2] $k_{O2} = 0.8 \times 10^{-14}$ cm^3 molecule^{-1} s^{-1}.

Bimolecular reaction rate constants of cyclohexoxy reaction with O_2 increase from 2.5×10^{-15} at 226 K to 2.1×10^{-14} cm^3 molecule^{-1} s^{-1} as the temperature is raised from 225 to 302 K. An Arrhenius plot of the data is shown in Figure 4. The uncertainties in the individual rate determinations are typically 8%, and the trend in the rate constant stands out clearly above

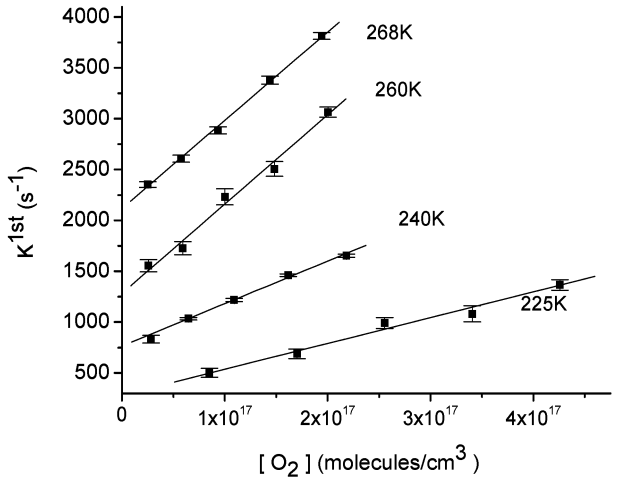

Figure 3. Linear fit of the pseudo-first-order rate constant versus the O_2 concentration for selected data at 225, 240, 260, and 268 K.

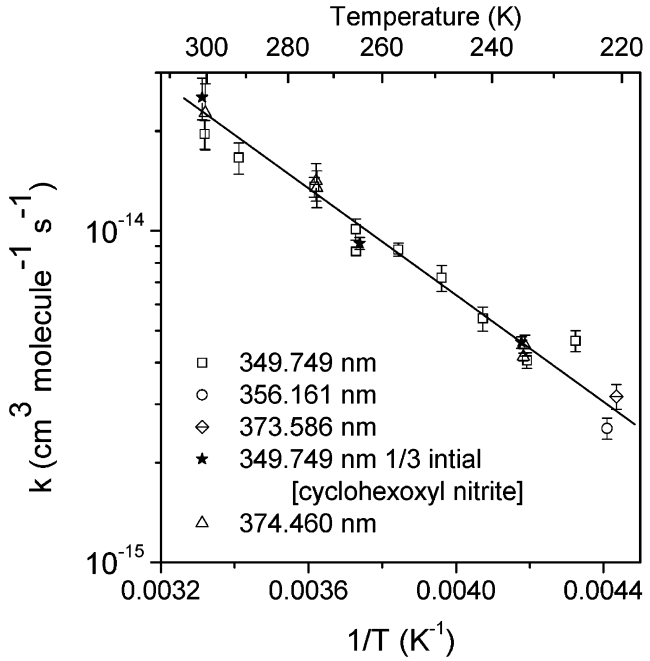

Figure 4. Arrhenius plot showing the temperature dependence of the rate constant for the reaction of cyclohexoxy with O_2.

the noise. By linearly fitting all the data in Figure 4, the Arrhenius expression is found to be

$$k_{O2} = (5.8 \pm 2.3) \times 10^{-12} \exp[(-14.3 \pm 0.8)\ \text{kJ/mol}/RT]\ \text{cm}^3\ \text{molecule}^{-1}\ \text{s}^{-1}\ (225-302\ \text{K})$$

where the cited errors represent two standard deviations of the statistical error. A summary of kinetic data for other alkoxy radical reactions with O_2 is listed in Table 2. Our Arrhenius preexponential factor of cyclohexoxy reaction with O_2 is 300−400 times larger than that for other secondary alkoxy radicals. Our activation energy is ∼6 kJ/mol larger than the next highest value (that for methoxy radical) and 9 times higher than that recommended for secondary alkoxy radicals.[2]

Since the temperature dependence measured here for the reaction of cyclohexoxy with O_2 is so very different from that expected for a secondary alkoxy radical, it is extremely important to consider possible sources of error. This reaction has the potential for extensive secondary chemistry. HO_2 is created by the abstraction reaction of O_2 (reaction 1). In the

TABLE 2: Arrhenius Parameters for the Reactions of Various Alkoxy Radicals with O_2

radical	A, cm^3 molecule^{-1} s^{-1}	E_a, kJ/mol	temp range, K	ref
CH_3O	55×10^{-15}	8.3	298−450	11
C_2H_5O	71×10^{-15}	4.6	295−411	13
	24×10^{-15}	2.7	295−354	18
1-C_3H_7O	14×10^{-15}	0.9	223−303	15
	25×10^{-15}	2.0	289−381	18
2-C_3H_7O	10×10^{-15}	1.8	218−313	15
	15×10^{-15}	1.6	298−383	12
	16×10^{-15}	2.2	288−364	18
2-C_4H_9O	1.25×10^{-15}	−4.6	221−266	25
	23×10^{-15}	1.4	223−305	54
3-pentoxy	4.1×10^{-15}	−2.6	220−285	25
cyclohexoxy	5850×10^{-15}	14.3	225−302	this work

presence of the NO generated by the photolysis of cyclohexyl nitrite, O_3 is produced:

$$HO_2 + NO \rightarrow OH + NO_2 \quad (2)$$

$$NO_2 + h\upsilon \rightarrow NO + O \quad (3)$$

$$O + O_2 + M \rightarrow O_3 + M \quad (4)$$

This chemistry is the same as that which produces O_3 in the polluted atmosphere. The presence of radicals such as OH, HO_2, and atomic oxygen give rise to concerns about secondary chemistry affecting the determination of k_{O2}. However, the three rate constants obtained using one-third the initial radical concentration (at 239, 267, and 302 K) are indistinguishable from those obtained at the higher radical concentration used in most of the experiments. This makes it extremely unlikely that secondary radical chemistry is affecting our determination of k_{O2}.

Another source of secondary chemistry is the accumulation of closed-shell (nonradical) reaction products such as cyclohexanone. The cyclohexyl nitrite flows along the paths of the photolysis and probe laser beams for ∼10 s before reaching the area which is in the viewing zone of the photomultiplier tube. To minimize accumulation of photoproducts, we repeated the experiments using a perpendicular alignment of photolysis and detecting lasers (at 238 K and 125 Torr). The rate constants are $(4.2 \pm 0.2) \times 10^{-15}$ cm^3 molecule^{-1} s^{-1} for counter-propagating alignment and $(4.5 \pm 0.7) \times 10^{-15}$ cm^3 molecule^{-1} s^{-1} for the perpendicular alignment, which is consistent within the error bars. Also, a single experiment was carried out at 276 K and 50 Torr in which the data acquisition frequency was increased from 2 to 3 Hz. The resulting rate constant of $(1.4 \pm 0.4) \times 10^{-14}$ cm^3 molecule^{-1} s^{-1} at 3 Hz is virtually the same as that obtained at 2 Hz: $(1.4 \pm 0.2) \times 10^{-14}$ cm^3 molecule^{-1} s^{-1}. These results further confirm that the rate constants reported here are not affected by secondary chemistry.

As noted previously and depicted in Figure 4, the kinetic experiments used four different excitation (detection) wavelengths. Results from all four wavelengths are consistent within the error bars. It is reasonable to conclude that all these peaks in the LIF spectrum arise from cyclohexoxy radical. This result is also consistent with our conclusion, based on the spectroscopic analysis, that all major peaks are due to a single conformer (axial).

The above discussion suggests no obvious sources of error that would explain the difference between the temperature dependence we observe for cyclohexoxy radical and that common to other secondary alkoxy radicals. If our observations are accurate, then the difference between the reactivity of O_2 with cyclohexoxy and with acyclic alkoxy radicals must have some physical/chemical basis. We note that cyclohexanone, which is the product of the O_2 reaction, possesses about 12 kJ/mol of strain energy, whereas cyclohexoxy radical, itself, is expected to have almost no strain energy.[41] If this amount of extra energy is present in the transition state for the O_2 reaction of cyclohexoxy and absent in the transition state for the O_2 reactions of acyclic alkoxy radicals, it would neatly explain the observed activation energy. It should be noted that tunneling is believed to contribute significantly, or even to dominate, the room-temperature rate constant,[39,40] so that the Arrhenius preexponential factor would be strongly affected by large changes in the activation barrier.

TABLE 3: B3LYP Absolute Energies (Hartrees) and Zero Point Energies (kJ/mol) of Transition States (TS) for β C−C Scission of Cyclohexoxy Radical, for O_2, and for products of the β C−C Scission and O_2 Reactions of Cyclohexoxy Radical

species	6-31G(d,p)	ZPE	6-311G (2df,2p)
TS scission (equatorial)	−310.419 936	413.4	−310.508 73
TS scission (axial)	−310.420 72	414.3	−310.509 62
6-oxo-1-hexyl radical	−310.429 23	406.8	−310.520 33
O_2	−150.319 13	9.9	−150.372 86
cyclohexanone	−309.905 25	396.8	−309.993 47
HO_2	−150.904 00	37.0	−150.959 19

3. Rate Constant for β C−C Scission. Tables 3 and 4 list absolute and relative energies for the β C−C scission of the axial and equatorial conformers of cyclohexoxy radical, and Figure 5 shows the potential energy profile for β C−C scission to produce 6-oxo-1-hexyl radical. The less stable axial conformer possesses a lower barrier to β C−C scission. We carried out RRKM/Master Equation calculations of the rate constant using the B3LYP/6-31G(d,p) activation energies, which have previously proven more reliable than those obtained with larger basis sets.[34−37,51] RRKM calculations suggest Arrhenius expressions for the C−C scission rate constant of the axial and equatorial conformers at 1 atm of N_2:

$$k_{\text{scission,axial}} = 2.0 \times 10^{13} \exp[-47.5 \text{ kJ/mol}/RT] \text{ s}^{-1}$$

$$k_{\text{scission,equatorial}} = 2.4 \times 10^{13} \exp[-50.5 \text{ kJ/mol}/RT] \text{ s}^{-1}$$

As with any computed rate constant, the activation barriers have considerable uncertainty, which we roughly estimate at 10 kJ/mol (2 sd). Figure 6 shows the pressure dependence of the rate constant for both conformers at 300 K; the pressure dependence is modest over range from 50 to 760 Torr. As the pressure drops from 760 to 50 Torr, the computed activation energy drops by 1−1.5 kJ/mol and the preexponential factor drops by a factor of 2−2.5.

Ideally, we could obtain C−C scission rate constants from experiment. One possible interpretation of the intercepts of our plots of k' versus $[O_2]$ (such as Figure 3) is that they represent the rate of β C−C scission of the cyclohexoxy radical. To evaluate this possibility, we plotted the natural logarithm of all the intercepts (of our plots of k' versus $[O_2]$) versus $1/T$ in Figure 7. Although the plot is consistent with an Arrhenius temperature dependence, the implied activation energy of ∼30 kJ/mol and preexponential factor of $10^{9.5\pm1.0}$ are far different than those obtained by our calculation. At room temperature and 50 Torr, the pseudo-first-order loss rate of about 1×10^4 s^{-1} is consistent with the rate of C−C scission of axial cyclohexoxy radical inferred from our computations (8×10^4 s^{-1}, with an uncertainty

TABLE 4: B3LYP Reaction Enthalpies (ΔH_r) and Activation Barriers (E_o) for β C−C Scission and O_2 Reaction of Cyclohexoxy Radical (kJ/mol)

	ΔH_r (0 K)		E_o	
reaction	6-31G(d,p)	6-311G(2df,2p)	6-31G(d,p)	6-311G(2df,2p)
β scission (equatorial)	17.3	3.5	48.2	40.5
β scission (axial)	15.6	2.4	45.4	38.0
equatorial + O_2 → cyclohexanone + O_2	−125.7	−135.7		

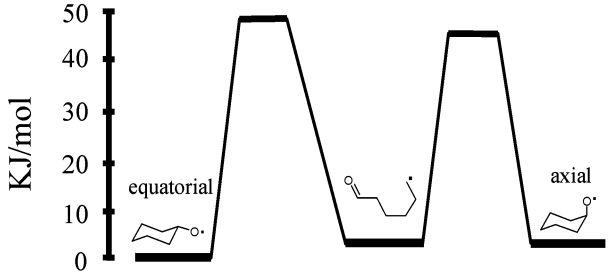

Figure 5. Potential energy profile for the β C−C scission of the equatorial and axial conformers of cyclohexoxy radical.

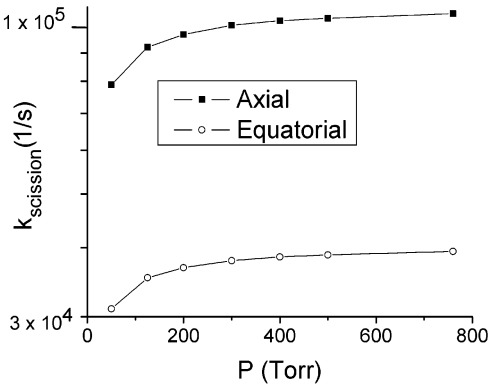

Figure 6. Pressure dependence of the rate constants for β C−C scission of the axial and equatorial conformers of cyclohexoxy radical at 300 K.

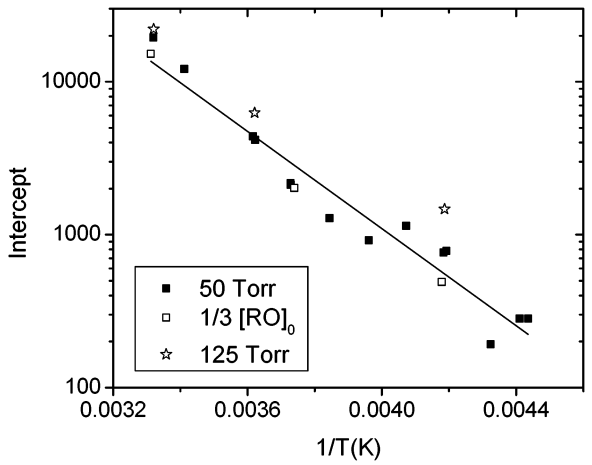

Figure 7. Arrhenius plot showing the temperature dependence of the intercepts of our plots of pseudo-first-order rate constant versus the O_2 concentration at two total pressures (50 and 125 Torr) and two concentrations of cyclohexyl nitrite at 50 Torr total pressure.

of at least a factor of 10). At lower temperatures, the intercepts are much higher than the computed rate of C−C scission. It is reasonable to think that C−C scission is contributing to the intercepts of our plots of k' versus $[O_2]$ but that other chemical losses must also be important, particularly at low temperatures.

Orlando, Iraci, and Tyndall[6] experimentally measured the ratio, $k_{O2}/k_{scission}$, of the reaction rate constants for O_2 reaction and β C−C scission for 273 K ≤ T ≤ 296 K:

$$k_{O2}/k_{scission} = (1.3 \pm 0.3) \times 10^{-27} \exp[(46.1 \pm 9.1)\ \text{kJ/mol}/RT]\ \text{cm}^3\ \text{molecule}^{-1}\ \text{s}^{-1}$$

TABLE 5: Experimental Pressure Dependence of the Rate Constant for Cyclohexoxy + O_2 at Three Temperatures

T, K	total pressure, Torr	K, cm^3 molecule^{-1} s^{-1}
239	50	$(4.2 \pm 0.1) \times 10^{-15}$
	125	$(4.5 \pm 0.3) \times 10^{-15}$
276	50	$(1.4 \pm 0.2) \times 10^{-14}$
	125	$(1.3 \pm 0.2) \times 10^{-14}$
301	50	$(2.0 \pm 0.2) \times 10^{-14}$
	125	$(2.3 \pm 0.5) \times 10^{-14}$

Based on this result and Atkinson's recommendation for the rate constant, $k_{O2} = 1.5 \times 10^{-14} \exp(-1.6\ \text{kJ/mol}/RT)$ cm^3 molecule^{-1} s^{-1}, Orlando et al., calculated the Arrhenius expression for the β C−C scission reaction rate constant as

$$k_{scission} = (1.2 \pm 0.3) \times 10^{13} \exp[-(47.7 \pm 9.1)\ \text{kJ/mol}/RT]\ \text{s}^{-1}$$

The agreement between our theoretical results and the analysis of Orlando, Iraci, and Tyndall is much better than could be expected given the significant uncertainties inherent in both values.

Just as Orlando, Iraci, and Tyndall use Atkinson's recommended value of k_{O2} to determine $k_{scission}$, the present experimental results can also be combined with Orlando et al.'s $k_{O2}/k_{scission}$ ratio to give

$$k_{scission} = (4.5 \pm 2.2) \times 10^{15} \exp[-(60.4 \pm 9.5)\ \text{kJ/mol}/RT]\ \text{s}^{-1}$$

The activation energy we infer from the relative rate measurement of Orlando, Iraci, and Tyndall is somewhat higher than the calculated value, but the difference is less than the combined uncertainties. However, because the Arrhenius preexponential for the O_2 reaction determined here is about 300 times larger than Atkinson's recommended value, the inferred Arrhenius preexponential factor for β C−C scission is about 300−400 times higher than that obtained by our theoretical calculation. This dramatic difference is very disconcerting!

Let us consider some possible causes for this discrepancy. The *A*-factor obtained by theory is very similar to those obtained from previous experimental and computational studies,[24,52] which strongly suggests that the error does not lie in the theoretical work. One possible explanation is that the rate constant for the cyclohexoxy + O_2 reaction, unlike those for other alkoxy radicals, is different at 50 Torr (where our measurements were made) than at 1 atm (where Orlando et al. made their measurements). We therefore remeasured the rate constant for the cyclohexoxy + O_2 reaction at 125 Torr at three temperatures, 239, 276, and 301 K. As can be seen from Table 5, the measured rate constant is essentially unchanged by this

increase in pressure. This result strongly suggests that the rate constant is not significantly different at 1 atm than at 50 Torr.

Another possible cause of this discrepancy arises from the presence of two conformers of cyclohexoxy radical or their interconversion on time scale of our experiment. Our experimental spectrum is consistent with the computed spectrum of the *axial* conformer of cyclohexoxy radical. In our experiments, the time scale for kinetic measurements is 5−400 μs. The barrier to axial−equatorial interchange (inversion) of substituted cyclohexanes (in solution) is about 45 kJ/mol and the Arrhenius preexponential factor is inferred to be 3×10^{13} s^{-1}.[41,53] At 225 K, the implied lifetime of the inversion reaction is ∼1 ms, so our observations are probably undisturbed by the interconversion. At 250 K and higher, the implied lifetime for the inversion reaction is comparable to, or shorter than, the time scale of our kinetic measurements (using rate parameters obtained from solution phase). However, if conformational interchange was affecting the concentration of the axial conformer, we would expect to see nonlinearities in some of our plots of ln(intensity) versus time or strongly non-Arrhenius behavior of the ln(k) versus 1/*T* plot. Since we observe neither of these behaviors, we conclude that conformational interchange is not affecting our kinetic results.

Let us take a closer look at the determinations of $k_{scission}$ from the relative rate data. The original data of Orlando, Iraci, and Tyndall consists of relative rate measurements at four temperatures in the range 273−296 K, each with uncertainties (2 sd) of ∼40%. The uncertainty they assigned to the Arrhenius preexponential factor was explicitly stated to be that of the 296 K data, rather than being derived from statistical analysis. Because of the limited temperature range spanned by the relative rate data, a more realistic estimate of the uncertainty in the fitted Arrhenius preexponential factor is a factor of 10. Another issue is that the results of the relative rate experiments necessarily reflect some averaging of the reactivity of both conformers. The two conformers could have significantly different rates of reaction with O_2, and our calculations suggest they have significantly different rates of β C−C scission reactions. Our spectra, and therefore, our kinetic results, seem to arise only from the less stable (axial) conformer; if so, it is not valid to combine our value of k_{O2} with the relative rate constants in order to extract a rate constant for C−C scission.

IV. Conclusion

We have reported the first observation of the LIF excitation spectrum of cyclohexoxy radical. The spectrum is consistent with a single conformer and comparison of the calculated and experimental spectrum suggests that the dominant features in the spectrum arise from the axial conformer of the cyclohexoxy radical. A direct study of the rate constant for cyclohexoxy radicals reacting with O_2 has been carried out using LIF to monitor the disappearance of cyclohexoxy radicals. The activation energy for k_{O2} is markedly higher than expected, a result which may arise from strain energy in the transition state.

Our theoretical calculation of the rate constant for β C−C scission, $k_{scission}$, is similar to that inferred by Orlando, Iraci, and Tyndall from their experimental measurement of $k_{O2}/k_{scission}$ and Atkinson's recommended k_{O2}. However, using our k_{O2} and Orlando's $k_{O2}/k_{scission}$, the calculated Arrhenius preexponential factor for $k_{scission}$ appears inconsistent with our calculations or with values found for other alkoxy radicals. The discrepancy between the Arrhenius preexponential factor derived from calculation and inferred by comparison of our k_{O2} and Orlando's $k_{O2}/k_{scission}$ is due, at least in part, to the uncertainty in the Arrhenius preexponential factor for $k_{O2}/k_{scission}$.

If our interpretation of the LIF spectra as being due to a single conformer is correct, it is not valid to compare our kinetic results to those of Orlando, Iraci, and Tyndall. A proper comparison would probably require knowledge of the temperature and pressure dependence of the rate of the axial−equatorial conversion in cyclohexoxy radical, confirmation (or correction) of our assignment of the spectrum to the axial conformer, and, perhaps, direct studies of the rate of the β scission reaction.

Acknowledgment. This research was supported by the National Science Foundation under Grant ATM-0087057 and by a Research Experience for Undergraduates supplement for K. A. K. This research was further supported by the National Computational Science Alliance under Grant ATM010003N, utilizing the HP-N4000 cluster at the University of Kentucky. We thank B. S. Hudson for the loan of the hardware for data acquisition, and J. Liu and T. A. Miller for permission to report a portion of their results prior to publication. We thank T. A. Miller and K. M. Callahan for helpful discussions, R. Atkinson, A. R. Ravishankara, S. P. Sander, and C. Anastasio for forcefully questioning our first explanations for the apparent discrepancy, and the anonymous reviewers for many very helpful comments.

References and Notes

(1) Atkinson, R. *J. Phys. Chem Ref. Data Monograph No. 2* **1994**.
(2) Atkinson, R. *Int. J. Chem. Kinet.* **1997**, *29*, 99.
(3) Jenkin, M. E.; Hayman, G. D. *Atmos. Environ.* **1999**, *33*, 1275.
(4) Schauer, J.; Kleeman, M.; Cass, G.; Simoneit, B. R. T. *Environ. Sci. Technol.* **2002**, *36*, 1169.
(5) Platz, J.; Sehested, J.; Nielsen, O. J. *J. Phys. Chem. A* **1999**, *103*, 2688.
(6) Orlando, J. J.; Iraci, L. T.; Tyndall, G. S. *J. Phys. Chem. A* **2000**, *104*, 5072.
(7) Aschmann, S. M.; Chew, A. A.; Arey, J.; Atkinson, R. *J. Phys. Chem. A* **1997**, *101*, 8042.
(8) Takagi, H.; Washida, N.; Bandow, H.; Akimoto, H.; Okuda, M. *J. Phys. Chem.* **1981**, *85*, 2701.
(9) Sanders, N.; Butler, J. E.; Pasternack, L. R.; McDonald, J. R. *Chem. Phys.* **1980**, *48*, 203.
(10) Gutman, D.; Sanders, N.; Butler, J. E. *J. Phys. Chem.* **1982**, *86*, 66.
(11) Lorenz, K.; Rhasa, D.; Zellner, R.; Fritz, B. *Ber. Bunsen-Ges. Phys. Chem.* **1985**, *89*, 341.
(12) Balla, R.; Nelson, H. H.; McDonald, J. R. *Chem. Phys.* **1985**, *99*, 323.
(13) Hartmann, D.; Karthauser, J.; Sawerysyn, J. P.; Zellner, R. *Ber. Bunsen-Ges. Phys. Chem.* **1990**, *94*, 639.
(14) Frost, M. J.; Smith, I. W. M. *J. Chem. Soc., Faraday Trans.* **1990**, *86*, 1757.
(15) Mund, C.; Fockenberg, C.; Zellner, R. *Ber. Bunsen-Ges. Phys. Chem.* **1998**, *102*, 709.
(16) Devolder, P.; Fittschen, Ch.; Frenzel, A.; Hippler, H.; Poskrebyshev, G.; Striebel, F.; Viskolcz, B. *Phys. Chem. Chem. Phys.* **1999**, *1*, 675.
(17) Caralp, F.; Devolder, P.; Fittschen, C.; Gomz, N.; Hippler, H.; Mereau, R.; Rayez, M. T.; Striebel, F.; Viskolcz, B. *Phys. Chem. Chem. Phys.* **1999**, *1*, 2935.
(18) Fittschen, C.; Frenzel, A.; Imrik, K.; Devolder, P. *Int. J. Chem. Kinet.* **1999**, *31*, 860.
(19) Wang, C.; Shemesh, L. G.; Deng, W.; Lilien, M. D.; Dibble, T. S. *J. Phys. Chem. A.* **1999**, *103*, 8207.
(20) Wang, C.; Deng, W.; Shemesh, L. G.; Lilien, M. D.; Katz, D. R.; Dibble, T. S. *J. Phys. Chem. A.* **2000**, *104*, 10368.
(21) Deng, W.; Wang, C. J.; Katz, D. R.; Gawinski, G. R.; Davis, A. J.; Dibble, T. S. *J. Phys. Chem. A* **2000**, *104*, 10368.
(22) Blitz, M.; Pilling, M. J.; Robertson, S. H.; Seakins, P. W. *Phys. Chem. Chem. Phys.* **1999**, *1*, 73.
(23) Fittschen, C.; Hippler, H.; Viskolcz, B. *Phys. Chem. Chem. Phys.* **2000**, *2*, 1677.
(24) Lotz, C.; Zellner, R. *Phys. Chem. Chem. Phys.* **2000**, *2*, 2353.
(25) Deng, W.; Davis, A. J.; Zhang, L.; Katz, D. R.; Dibble, T. S. *J. Phys. Chem. A.* **2001**, *105*, 8985.
(26) Carter, C. C.; Gopalakrishnan, S.; Atwell, J. R.; Miller, T. A. *J. Phys. Chem. A* **2001**, *105*, 2925.
(27) Gopalakrishnan, S.; Carter, C. C.; Zu, L.; Stakhursky, V.; Tarczay, G.; Miller, T. A. *J. Chem. Phys.* **2003**, *118*, 4954.

(28) Gopalakrishnan, S.; Zu, L.; Miller, T. A. *J. Phys. Chem A* **2003**, *107*, 5189.

(29) Blatt, A. H. *Organic Syntheses*; Wiley: New York, 1966; pp 108−109.

(30) Typical alkylnitrite IR and NMR spectra may be found in the Sadtler Index, Bio-Rad Laboratories Inc., 1973.

(31) Frisch, M. J.; Trucks, G. W.; Schlegel, H. B.; Gill, P. M. W.; Johnson, B. G.; Robb, M. A.; Cheeseman, J. R.; Keith, T.; Petersson, G. A.; Montgomery, J. A.; Raghavachari, K.; Al-Laham, M. A.; Zakrzewski, V. G.; Ortiz, J. V.; Foresman, J. B.; Cioslowski, J.; Stefanov, B. B.; Nanayakkara, A.; Challacombe, M.; Peng, C. Y.; Ayala, P. Y.; Chen, W.; Wong, M.; Andres, J. L.; Replogle, E. S.; Gomperts, R.; Martin, R. L.; Fox, D. J.; Binkley, J. S.; Defrees, D. J.; Baker, J.; Stewart, J. P. Head-Gordon, M. Gonzalez, C. Pople, J. A. Gaussian98, Revision D.3 Gaussian, Inc.: Pittsburgh, PA, 1995.

(32) Lee, C.; Yang, W.; Parr, R. G. *Phys. Rev. B* **1988**, *37*, 785.

(33) Becke, A. D. *J. Chem. Phys.* **1993**, *98*, 5648.

(34) Orlando, J. J.; Tyndall, G. S.; Bilde, M.; Ferronato, C.; Wallington, T. J.; Vereecken, L.; Peeters, J. *J. Phys. Chem. A* **1998**, *102*, 8116.

(35) Dibble, T. S. *J. Phys. Chem. A* **1999**, *103*, 8559.

(36) Dibble, T. S. *Chem. Phys. Lett.* **1999**, *301*, 297.

(37) Peeters, J.; Fantechi, G.; Vereecken, L. *J. Atmos. Chem.*, submitted 2003.

(38) Gilbert, R. G.; Smith, S. C.; Jordan, M. J. T. UNIMOL program suite (calculation of falloff curves for unimolecular and recombination reactions), 1993. Available from the authors: School of Chemistry, Sydney University, NSW 2006, Australia. E-mail: gilbert_r@summer.chem.su.oz.au.

(39) Bofill, J. M.; Olivella, S.; Solé, A.; Anglada, J. M. *J. Am. Chem. Soc.* **1999**, *121*, 1337.

(40) Setokuchi, O.; Sato, M. *J. Phys. Chem. A* **2002**, *106*, 8124.

(41) Eliel, E. L.; Wilen, S. H. *Stereochemistry of Organic Compounds*; Wiley: New York, 1994.

(42) Powers, D. E.; Pushkarsky, M.; Miller, T. A. *J. Chem. Phys.* **1997**, *106*, 6863.

(43) Tan, X. Q.; Williamson, J. M.; Foster, S. C.; Miller, T. A. *J. Phys. Chem.* **1993**, *97*, 9311.

(44) Foster, S. C.; Misra, P.; Lin, T. Y.; Damo, C. P.; Carter, C. C.; Miller, T. A. *J. Phys. Chem.* **1988**, *92*, 5914.

(45) Liu, X.; Damo, C. P.; Lin, T. Y.; Foster, S. C.; Mistra, P.; Yu, L.; Miller, T. A. *J. Phys. Chem.* **1989**, *93*, 2266.

(46) Powers, D. E.; Pusharsky, M.; Miller, T. A. *J. Phys. Chem.* **1997**, *106*, 6863.

(47) Inoue, G.; Akimoto, H.; Okuda, M. *Chem. Phys. Lett.* **1979**, *63*, 213.

(48) Ohbayashi, K.; Akimoto, H.; Tanaka, I. *J. Phys. Chem.* **1977**, *81*, 798.

(49) Wendt, H. R.; Hunziker, H. E. *J. Phys. Chem.* **1979**, *71*, 5202.

(50) Liu, J.; Miller, T. A., manuscript in preparation.

(51) Jungkamp, T. P. W.; Smith, J. N.; Seinfeld, J. H. *J. Phys. Chem. A* **1997**, *101*, 4392;

(52) Devolder, P. *J. Photochem. Photobiol A* **2003**, *157*, 137.

(53) Carey, F. A.; Sundberg, R. J. *Advanced Organic Chemistry*, 2nd ed.; Part A: structure and mechanisms.

(54) Zellner, R.; Lotz, Ch. In *Transport and Chemical Transformation in the Troposphere, Proceedings of the 7th EUROTRAC Symposium*, 2002; Midgley, P.M., Reuther, M., Eds.; pp 464−467.